On amphicheiral knots

Chengzhi Liang and Kurt Mislow

Department of Chemistry, Princeton University,
Princeton, NJ 08544, USA

Amphicheiral knots with up to 12 crossings are discussed from the perspective of their symmetry properties. By use of an algorithm that involves the development of appropriate vertex-bicolored knot graphs, rigidly achiral presentations have been found for all amphicheiral invertible prime knots with up to 10 crossings and for a selected number of such knots with 12 crossings, including 12_{1994}, the first example of an amphicheiral prime knot whose S_{2n} diagram is also a reduced diagram. Characteristic properties of wire models of these presentations have been examined. The adjacency matrices of the vertex-bicolored graphs of amphicheiral knots exhibit twofold antisymmetry, and, with the sole exception of 12_{427}, all such knots are capable of rigidly antisymmetric presentations.

1. Introduction

Knotted molecules are exotic newcomers on the scene in chemistry and biochemistry. Single- and double-stranded DNA knots, though arguably present in living organisms millions of years ago, were first discovered in 1976 [1]; by now they have become a commonplace in "biochemical topology" [2–4]. The rational synthesis of molecular knots – suggested as long ago as 1953 [5], and the subject of ingenious proposals in the 1970s [6] – was finally achieved in 1989 [7]. This milestone in "chemical topology" [8,9] and "topological stereochemistry" [10,11] was followed in 1991 by the first rational synthesis of single-stranded DNA knots [12]. But fascination with knotted objects transcends their embodiment in molecular form: their universal appeal lies in the apparently limitless capacity of knots to adopt intricately interlaced and convoluted structures, in the dazzling symmetry of these structures (as in the magnificent Celtic knotwork [13]), and in the mathematical challenges posed by the resulting complexity. Knots and links thus afford a rich source of intellectual and aesthetic delight to chemists and mathematicians alike.

In this article we report some observations on amphicheiral knots, a class of knots whose allure derives from their special symmetry. To provide the necessary background, we begin our account with an informal description of some basic con-

cepts and terminology; for further details the reader is referred to the specialized literature [14–24].

A *knot* is a closed curve embedded in 3-space that does not intersect itself. Accordingly, a circle in the plane is also a knot, though a trivial one (the *unknot*). A given knot can be distorted, by continuous deformations, into a variety of shapes (*presentations*) that form an equivalence class (*isotopy type*). Equivalent presentations are *isotopic* or *homeotopic*; the latter term may be preferable in a chemical context since the former carries a totally different meaning in chemistry [11c].

For convenience in analysis, knots are projected in the plane as *knot diagrams*: closed curves in which each transverse double point is marked in a suitable manner so as to represent an over- or an undercrossing, as illustrated in fig. 1(a) and (b)
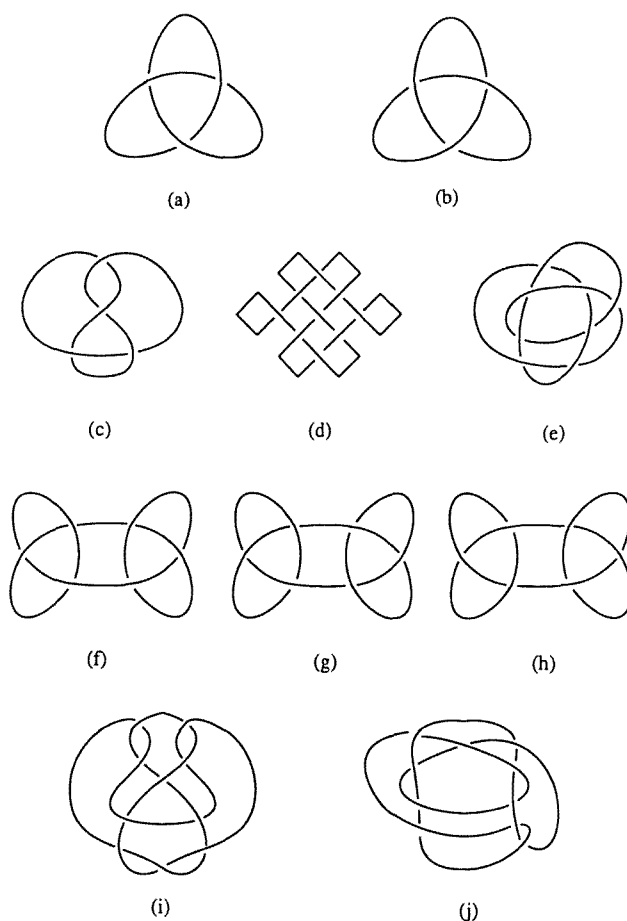
Fig. 1. (a) and (b) Enantiomorphs of the trefoil or overhand knot, 3_1. (c) Figure-eight, or Listing's, knot, 4_1. (d) Knot 7_4, with two nugatory crossings. (e) A non-alternating knot, 8_{20}. (f) Square, or reef, knot. (g) and (h) Enantiomorphs of the granny knot. (i) and (j) The "Perko pair", with writhes +8 and +10.

for the two mirror-image forms (*enantiomorphs*) of the trefoil, or overhand, knot. Crossing points in knot diagrams are characterized by first assigning a direction to, i.e. orienting, the curve – the choice of direction is immaterial – and then labeling the crossing points with the appropriate signs in accordance with the convention in fig. 2. Thus, all three crossings are positive in fig. 1(a) and negative in fig. 1(b). Note that while each crossing point is always associated with a two-valued *characteristic*, ϵ, the assumption of a numerical value as in fig. 2 is not an exclusive option, as will be shown below.

The number of crossings in a knot diagram may be reduced to a minimum by removal of all unnecessary or *nugatory* crossings, to yield a *reduced diagram* . For a knot K that number is the *minimum crossing number, $c(K)$ (crossing number*, for short). For example, $c(K) = 0$ for the unknot, 3 for the trefoil knot, 4 for the figure-eight, or Listing's, knot (fig. 1(c)), and 7 for the knot in fig. 1(d), which has two nugatory crossings and which is "one of the eight glorious emblems of Tibetan Buddhism" [24]. Knot types are characterized by their crossing numbers according to a convention [14,25] in which $c(K)$ is subscripted by a numerical index, needed because two or more nonequivalent knots share the same crossing number for $c(K) > 4$. For example, the knots depicted in fig. 1(a), (b), (c), (d), and (e) are denoted 3_1, 3_1, 4_1, 7_4, and 8_{20}, respectively. The *writhe*, $w(K)$, of a knot K is the arithmetic sum of the crossing point characteristics, each of which has a value of $+1$ or -1, i.e., $w(K) = \Sigma\epsilon$. For example, the writhes of the knots depicted in fig. 1(a), (b), (c), (d), and (e) are $+3, -3, 0, +7$, and -2, respectively. A knot is *alternating* if overpasses alternate with underpasses all along the curve in the reduced knot diagram; otherwise it is *non-alternating*. For example, $3_1, 4_1$, and 7_4 are alternating knots, while 8_{20} is non-alternating. Alternating knots are listed first in knot tabulations, followed by non-alternating knots.

Also shown in fig. 1 are the square, or reef, knot, (f), and the two enantiomorphs of the granny knot, (g) and (h), with $w(K) = 0, +6$, and -6, respectively. In each knot, a plane perpendicular to the plane of projection and pierced in exactly two points cuts the knot in half. If the open ends on both sides of the plane are now joined to form closed curves, two trefoil knots result. The square and granny knots are examples of *composite* or *product knots*, $K_1 \# K_2$, whose factors are *prime knots*. For examples, if 3_1 denotes the enantiomorph with a positive and 3_1^* the one with a negative writhe, then (f) $= 3_1 \# 3_1^* = 3_1^* \# 3_1$, (g) $= 3_1 \# 3_1$, and (h) $= 3_1^* \# 3_1^*$. In contradistinction, $3_1, 4_1, 7_4$, and 8_{20} are all prime knots since they cannot be

(+)   (−)
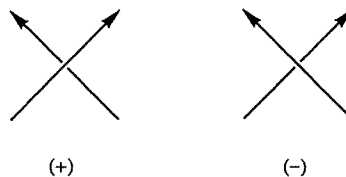
Fig. 2. Convention used to assign characteristics ($\epsilon = +1$ or -1) to crossings in knot diagrams.

divided (factored) into smaller, non-trivial knots. Chemists will have no difficulty recognizing that the square knot is in some ways analogous to the meso diastereomer of a compound such as 2,3-dibromobutane, while the enantiomorphs of the granny knot are analogous to the D and L isomers [26].

Tables and projections of alternating and non-alternating prime knots with up to 10 crossings were compiled toward the end of the nineteenth century by a "trio of tabulating titans" [20]: Kirkman [27], Little [28], and Tait [29]. This count (*census*) of the "classical knots" stood the test of time until 1974, when Perko showed that two non-alternating knots with *different* writhes (10_{161} and 10_{162} in [24] after reflection of one of the diagrams) were in fact isotopic. Called "notorious" [20], and even "infamous" [30], the "Perko pair" is shown in fig. 1(i) and (j). The most recent census is by Thistlethwaite [20], who lists 12,965 prime knots with up to 13 crossings, but adds the cautionary note that "it would be most unwise to claim categorically that this listing was correct, in the absence of independent verification".

2. Topological chirality and achirality

A knot is topologically achiral, or *amphicheiral*, if and only if it can be mapped onto its mirror image by a continuous (isotopic) deformation; otherwise it is topologically chiral. Topological chirality and achirality have been of central concern since the dawn of knot theory [31], and interest in this topic continues unabated; for example, see [30,32–38] and references cited above.

Amphicheiral knots are vastly outnumbered by chiral ones: of the 12,965 prime knots with $c(K) \leqslant 13$, only 78 are amphicheiral. As is evident upon inspection of the census in table 1, one reason is that the total count of knots increases steeply with

Table 1
Census of prime knots.

Crossing number	Total number of knots [a]	Number of amphicheiral knots
3	1	0
4	1	1
5	2	0
6	3	1
7	7	0
8	21	5
9	49	0
10	165	13
11	552	0 [b]
12	2 176	58 [b]
13	9 988	0 [b]

[a] [20]. Chiral knots are counted only once.
[b] [53].

an increase in crossing number while the fraction of amphicheirals decreases almost exponentially. That is, the density of amphicheirals decreases as the crossing number increases. The second reason is that no amphicheiral knot with an odd crossing number has ever been encountered. Tait [29] conjectured that all knots with an odd crossing number are topologically chiral, and just over a hundred years later Murasugi [39] proved Tait's conjecture to be true for alternating knots. Hence, all amphicheiral alternating knots have an even number of crossings. Furthermore, it was proven [33b,40] that the reduced diagrams of such knots have a writhe of zero, i.e., an equal number of over- and undercrossings that are switched upon reflection in the plane of projection. It is truly remarkable that this was anticipated in Tait's empirical studies, and that Tait also correctly identified all amphicheiral prime knots with up to 10 crossings: 4_1; 6_3; 8_3, 8_9, 8_{12}, 8_{17}, 8_{18}; 10_{17}, 10_{33}, 10_{37}, 10_{43}, 10_{45}, 10_{79}, 10_{81}, 10_{88}, 10_{99}, 10_{109}, 10_{115}, 10_{118}, 10_{123} (in modern notation). All these knots are alternating.
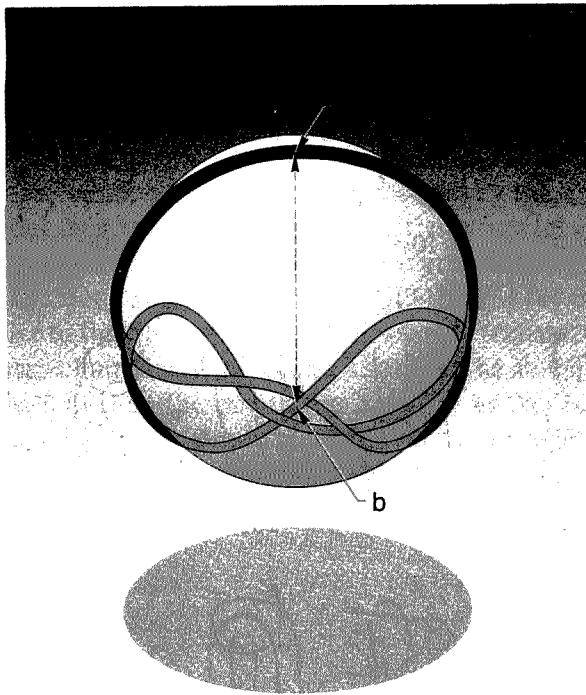
Fig. 3. Knot 6_3 symmetrically stretched over a sphere. The dashed line is a diameter that connects the midpoints a and b of the two laps at the antipodes of the sphere.
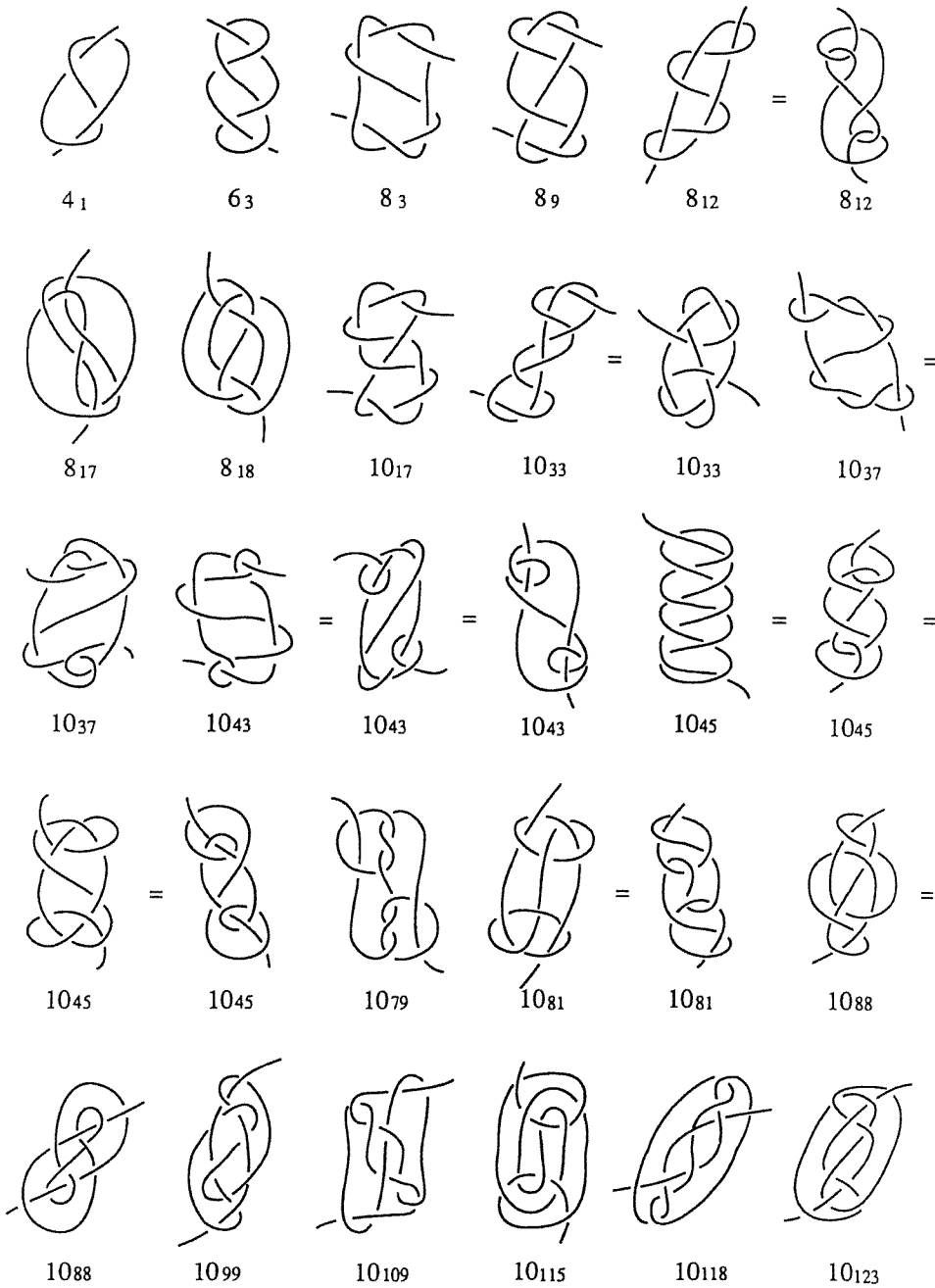
Fig. 4. Tait diagrams for the 20 amphicheiral prime knots with up to 10 crossings. The equal signs connect some alternative choices of antipodal laps for the same knot. See also fig. 5.

In the course of his investigations, Tait [29c] noted that every amphicheiral prime knot with up to 10 crossings can be "symmetrically stretched over a sphere", with the midpoints of two laps disposed antipodally as illustrated for 6_3 in fig. 3; the term "lap" as used here refers to a segment or arc of the knot whose ends are given by two consecutive crossings. If one the laps is cut at the midpoint, as at a or b in fig. 3, and the opened knot is projected on a plane, a centrosymmetric reduced diagram is obtained. Such diagrams (which we propose to call *Tait diagrams*) are shown in fig. 4 for the 20 classical amphicheiral prime knots.

How is one to describe the "quasi-symmetry" [29c] of presentations such as the one in fig. 3? If symmetry operations are restricted to the classical combinations of rotations and reflections, i.e., to strictly geometric operations, then the presentation in fig. 3 is clearly asymmetric. What is needed to capture the essence of the "quasi-symmetry" is an additional, non-geometric operation that switches over- and undercrossings. This purpose is served by the dichromatic operation [41], in which two colors are used to represent over- and undercrossings [42]. Seen in this light, Tait's pairs of "right and left handed meshes" [29c] are related as a right-handed black glove and a right-handed white glove (or a left-handed black glove and a left-handed white glove), and Tait's "quasi-symmetry" finds expression in a Shubnikov dichromatic point group [41]. For the 20 knots in fig. 4 this group is $C_2' = \{e, C_2'(x)\}$, where $C_2'(x)$ denotes the operation of twofold antirotation, i.e. rotation by π around the x-axis *combined* with a transposition of colors. The x-axis, or twofold axis of antisymmetry, which is represented by the dashed line in fig. 3, bisects the antipodal laps and thus contains exactly two points that belong to the knot. Alternatively, twofold antirotation can be expressed in isomorphic permutation groups $G' \cong C_2'$. For example, $G' = \{e, (12)(34)(56)'\}$ for 6_3, where the numbered crossings refer to fig. 5 and the prime indicates the transposition of colors.

Whereas all classical amphicheiral prime knots can be shaped into *rigidly antisymmetric presentations*, like the one in fig. 3, chiral knots, *including* those with writhe 0 (e.g. 8_4, 10_{19}, 10_{31}, and 10_{91}, to mention just a few), are incapable of adopting such presentations. These observations suggest that twofold antisymmetry is a stronger condition for amphicheirality than writhe.
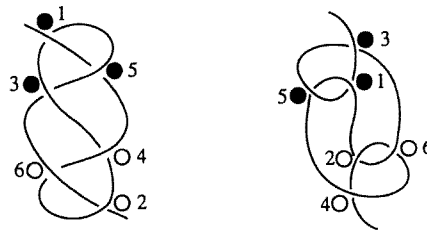
Fig. 5. Tait diagrams of knot 6_3 with numbered crossings. The filled (black) and open (white) circles correspond to $\epsilon = +1$ and -1, respectively. Left: cut at a in fig. 3. Right: cut at b in fig. 3.

3. Vertex-bicolored knot graphs of antisymmetric presentations

To each reduced diagram of a knot may be associated a planar multigraph (a *knot graph*) whose vertices and edges represent the knot's crossing points and laps. A graph is a knot graph if and only if (a) it is regular of degree 4, (b) it consists of a single block, and (c) the path created by joining the ends of opposite edges at each vertex is a single closed curve ("eulerian trail") [43].

3.1. VERTEX-BICOLORED GRAPHS

Different knots can have the same knot graph; for example, $8_{17}, 8_{19}, 8_{20},$ and 8_{21} all have the same graph [43]. This degeneracy is lifted if each vertex is labeled with a suitable characteristic that differentiates over- from undercrossings. For example, use of filled (black) and open (white) circles to label the vertices yields *vertex-bicolored knot graphs*, $G(K)$ [42]; these graphs differentiate the four knots from each other and the three chiral knots, $8_{19}, 8_{20},$ and $8_{21},$ from their non-isotopic enantiomorphs (fig. 6). In contradistinction, the graphs of the amphicheiral knot 8_{17} and its mirror image are isomorphic; that is, their adjacency matrices are the same. That $w(8_{17}) = 0$ is immaterial; for example, in the case of chiral 8_4, whose writhe is also zero, the vertex-bicolored graphs of the enantiomorphs are *not* isomorphic. What matters instead is whether the black and white subgraphs and the connectivities between them are equivalent: if they are, then the graphs of the mirror-image diagrams are isomorphic, otherwise they are not. For example, 10_{43} is an amphicheiral knot whose diagram in Rolfsen's table [24] is reproduced in fig. 7(a). Because the black and white subgraphs of the associated graph G(a) are not equivalent, G(a) is not isomorphic to its mirror image (the mirror image is obtained by switching the colors, which corresponds to a reflection in the plane). Continuous deformation yields the diagram in fig. 7(b), whose associated graph, G(b), *is* isomorphic to its mirror image because the black and white subgraphs and the connectivities between them are equivalent. G(b) can be converted into a Tait diagram (fig. 4) by cutting one of the two laps that corresponds to the edges between vertices 1 and 10 and vertices 4 and 7. The duality described for 10_{43} is not unique and is shared by the diagrams for 10_{81} and 10_{88} in Rolfsen's table.

3.2. ADJACENCY MATRICES

The distinction between the two diagrams in fig. 7 is also expressed in the adjacency matrices, $\mathbf{A}$, of the respective vertex-bicolored graphs. Following precedent [42], we define the adjacency matrix $\mathbf{A} = (a_{ij})$ as one whose elements are given by

$$a_{ii} = \begin{cases} t & \text{if vertex } i \text{ is black,} \\ t^{-1} & \text{if vertex } i \text{ is white,} \end{cases}$$
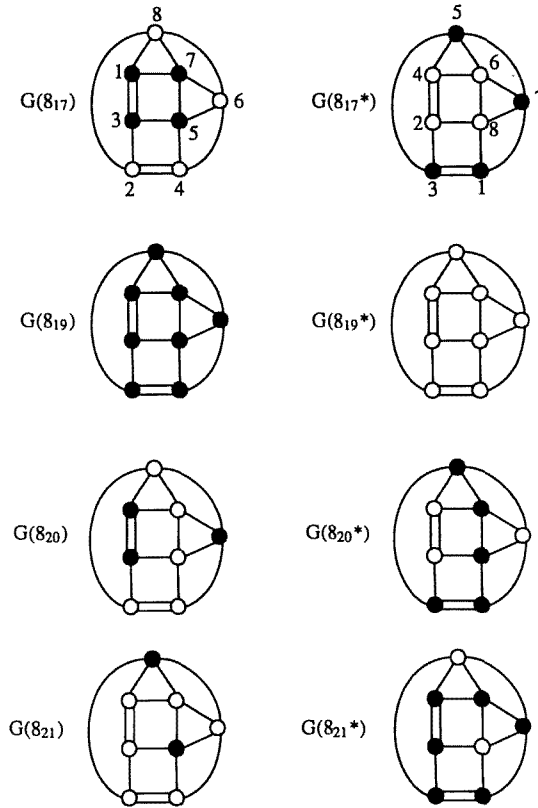
Fig. 6. Seven different knots with the same knot graph but with different vertex-bicolored graphs: $8_{17} \cong 8_{17}^*, 8_{19}, 8_{19}^*, 8_{20}, 8_{20}^*, 8_{21}$, and 8_{21}^* (8_x^* is the mirror image of 8_x). The amphicheiral knot 8_{17} and its mirror image 8_{17}^* have identical connectivities, as indicated by the numbered vertices.
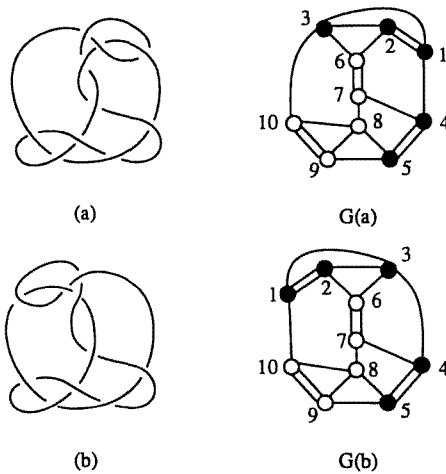
Fig. 7. Two reduced diagrams of 10_{43} and associated vertex-bicolored knot graphs. Diagram (b) corresponds to an antisymmetric presentation whereas diagram (a) [24] does not. Graph G(b) is isomorphic to its mirror image whereas graph G(a) is not.

$$a_{ij} = \begin{cases} s & \text{vertices } i \text{ and } j \text{ are connected with multiplicity } s, \\ 0 & \text{otherwise}. \end{cases}$$

The absolute value of t satisfies $|t| \neq 1$. Accordingly, with reference to G(a) and G(b) in fig. 7:

$$\mathbf{A}(a) = \begin{pmatrix}
t & 2 & 1 & 1 & 0 & 0 & 0 & 0 & 0 & 0 \\
2 & t & 1 & 0 & 0 & 1 & 0 & 0 & 0 & 0 \\
1 & 1 & t & 0 & 0 & 1 & 0 & 0 & 0 & 1 \\
1 & 0 & 0 & t & 2 & 0 & 1 & 0 & 0 & 0 \\
0 & 0 & 0 & 2 & t & 0 & 0 & 1 & 1 & 0 \\
0 & 1 & 1 & 0 & 0 & t^{-1} & 2 & 0 & 0 & 0 \\
0 & 0 & 0 & 1 & 0 & 2 & t^{-1} & 1 & 0 & 0 \\
0 & 0 & 0 & 0 & 1 & 0 & 1 & t^{-1} & 1 & 1 \\
0 & 0 & 0 & 0 & 1 & 0 & 0 & 1 & t^{-1} & 2 \\
0 & 0 & 1 & 0 & 0 & 0 & 0 & 1 & 2 & t^{-1}
\end{pmatrix}$$

$$\mathbf{A}(b) = \begin{pmatrix}
t & 2 & 1 & 0 & 0 & 0 & 0 & 0 & 0 & 1 \\
2 & t & 1 & 0 & 0 & 1 & 0 & 0 & 0 & 0 \\
1 & 1 & t & 1 & 0 & 1 & 0 & 0 & 0 & 0 \\
0 & 0 & 1 & t & 2 & 0 & 1 & 0 & 0 & 0 \\
0 & 0 & 0 & 2 & t & 0 & 0 & 1 & 1 & 0 \\
0 & 1 & 1 & 0 & 0 & t^{-1} & 2 & 0 & 0 & 0 \\
0 & 0 & 0 & 1 & 0 & 2 & t^{-1} & 1 & 0 & 0 \\
0 & 0 & 0 & 0 & 1 & 0 & 1 & t^{-1} & 1 & 1 \\
0 & 0 & 0 & 0 & 1 & 0 & 0 & 1 & t^{-1} & 2 \\
1 & 0 & 0 & 0 & 0 & 0 & 0 & 1 & 2 & t^{-1}
\end{pmatrix}$$

A twofold axis of antisymmetry may be imagined to pass through the center (i.e., the intersection of the major and minor axes) of A(b), at right angles to the paper. There is no such axis in A(a). In general, twofold antisymmetry in A satisfies the following relationship:

$$a_{ii} \leftrightarrow a_{N+1-i, N+1-i},$$

$$a_{ij} = a_{N+1-j, N+1-i},$$

where $i, j = 1, 2, \ldots, N$, and $\leftrightarrow$ represents a switch in colors. It should be noted that the four 1's in the minor diagonal of A(b) represent the two edges in G(b) that correspond to the two laps bisected by the twofold axis of antisymmetry. Exactly four 1's are found in the minor diagonals of all the antisymmetric adjacency matrices of the 20 amphicheiral prime knots with up to 10 crossings.

For any random labeling of vertices, the adjacency matrix, $\mathbf{A}'$, can always be converted into one with twofold antisymmetry, $\mathbf{A}$, by the appropriate transformation, $\mathbf{A} = \mathbf{T}\mathbf{A}'\mathbf{T}^{-1}$, *provided* that the black and white subgraphs of the corresponding vertex-bicolored graph (and the connectivities between them) are equivalent, as in G(b). On the other hand, because the black and white subgraphs of G(a) are not equivalent, it is not possible to transform $\mathbf{A}$(a) into a matrix that exhibits twofold antisymmetry, even though the diagrams in fig. 7(a) and (b) project equivalent (isotopic) presentations of the same knot.

3.3. POLYNOMIALS DERIVED FROM ADJACENCY MATRICES

For diagrams with twofold antisymmetry, $P(t) = P(t^{-1})$, where $P(t)$ is defined [42] as

$$P(t) = \det(\mathbf{A}).$$

For example, for the diagram in fig. 7(b):

$$P(t) = P(t^{-1}) = -16t^{-5} + 12t^{-4} + 192t^{-3} - 288t^{-2} - 368t^{-1} + 936$$
$$- 16t^5 + 12t^4 + 192t^3 - 288t^2 - 368t.$$

On the other hand, $P(t) \neq P(t^{-1})$ for the diagram in fig. 7(a):

$$P(t) = -16t^{-5} + 3t^{-4} + 180t^{-3} - 246t^{-2} - 360t^{-1} + 967$$
$$- 16t^5 + 4t^4 + 200t^3 - 200t^2 - 516t,$$

$$P(t^{-1}) = -16t^{-5} + 4t^{-4} + 200t^{-3} - 200t^{-2} - 516t^{-1} + 967$$
$$- 16t^5 + 3t^4 + 180t^3 - 246t^2 - 360t.$$

The fundamental task of the theory of knots was stated over a hundred years ago by its foremost pioneer: "Given the number of its double points, to find all the essentially different forms which a closed curve can assume" [29a]. To meet this objective requires the development of *knot invariants*, mathematical objects, such as knot groups or topological spaces, that can be unambiguously assigned to knot types. The crossing number is an example of a weak knot invariant since different knots may share the same number (table 1). Is the polynomial $P(t)$ a knot invariant?

The first polynomial knot invariant, discovered by Alexander in 1928 [44], failed to distinguish between enantiomorphs. This problem was overcome in 1985 by the Jones polynomial [45]. Jones' discovery triggered a burst of activity that led to more powerful, two-variable polynomials [36,37,46,47], all of which have in common a key feature that is also shared by $P(t)$: under transposition of t and t^{-1}, the polynomial remains unchanged if the knot is amphicheiral. However, while the Jones, Homfly, and Kauffman polynomials are independent of any particular presentation or projection, this is not true for $P(t)$: as the example of 10_{43} demon-

strates, $P(t) = P(t^{-1})$ for an amphicheiral knot only if the adjacency matrix of the vertex-bicolored graph has twofold antisymmetry (or can be transformed into one that does). Otherwise $P(t) \neq P(t^{-1})$, a condition that is not sufficient to allow a distinction to be made between an amphicheiral and a non-amphicheiral knot. In short, $P(t)$ depends for its success on the "correct" choice of a projection, and it follows that this polynomial cannot be a knot invariant.

These observations lead to the following conjecture: a knot is amphicheiral if and only if *at least one* of the polynomials derived from its vertex-bicolored graphs satisfies $P(t) = P(t^{-1})$, the condition of twofold antisymmetry; otherwise it is topologically chiral. Although we know of no exceptions, we are aware that there may be room for surprises akin to the failure of the Jones polynomial to detect the chirality of 9_{42} [37].

4. Presentations with geometric symmetry

Some knots are capable of attaining presentations with geometric symmetry. Such *rigidly symmetric presentations* are exemplified by the trefoil, figure-eight, square, and granny knots, which are shown in fig. 1 with D_3, C_2, C_{2h}, and D_2 symmetry, respectively. Nor are such presentations necessarily unique; for example, the trefoil knot can also display D_2 symmetry.

Thirteen of the 20 amphicheiral prime knots with up to 10 crossings (4_1, 6_3, 8_3, 8_9, 8_{12}, 8_{18}, 10_{17}, 10_{33}, 10_{37}, 10_{43}, 10_{45}, 10_{99}, 10_{123}) can attain rigidly symmetric presentations with twofold axes of rotation, though in some cases this may require the addition of nugatory crossings (fig. 8). Rotation by π around the twofold axis reverses the knot's orientation, i.e., the direction given by an arrow along the curve. Each of these *invertible knots* [15,16,35] can therefore be isotoped to one whose orientation has been reversed. Note that rotation by π *combined* with reversal of orientation is an operation that is abstractly equal to twofold antirotation (section 2.2), with orientation taking the place of color.

The remaining seven non-invertible knots (8_{17}, 10_{79}, 10_{81}, 10_{88}, 10_{109}, 10_{115}, 10_{118}) are asymmetric in all of their presentations [19] and hence, in contrast to invertible knots, cannot attain *rigidly achiral presentations* [33]. It follows that interconversion of enantiomorphous presentations by continuous deformation cannot proceed through a rigidly achiral state. Although interconversion of enantiomorphous presentations of invertible knots *can* proceed through such a state, there are an infinite number of interconversion paths by which this state can be circumvented (as illustrated for 4_1 in fig. 7 of [16], fig. 11 of [22], and scheme 35 of [11b]). Because of the absence of a boundary set of rigidly achiral presentations, enantiomorphous presentations of invertible as well as non-invertible amphicheiral prime knots cannot be partitioned into heterochiral classes.
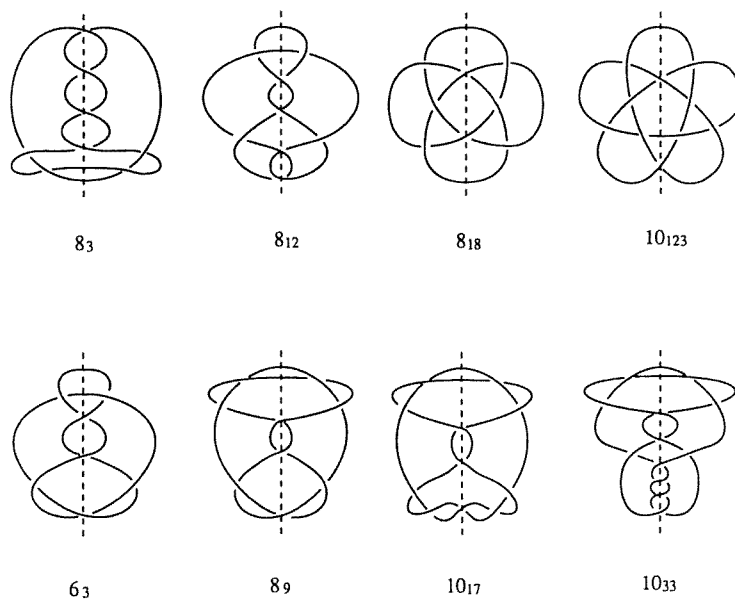
Fig. 8. A sampling of invertible amphicheiral prime knots in presentations with twofold axes of rotation (dashed lines). Top: reduced diagrams. Bottom: diagrams with additional nugatory crossings. Only one of the multiple twofold axes is shown for 8_{18} and 10_{123}.

4.1. FROM KNOT GRAPHS TO RIGIDLY ACHIRAL PRESENTATIONS

A rigidly achiral presentation of a prime knot cannot contain a plane of symmetry, for if the plane were the plane of projection, reflection would switch over- and undercrossings, and if the plane were perpendicular to the plane of projection, the knot would not be prime. This leaves $S_{2n}, n = 1, 2, \ldots$, as the only possible point group for such presentations.

We have found it convenient to use a simple pictorial algorithm to develop rigidly achiral presentations. The algorithm consists of the following four steps: (1) choose a knot graph that is compatible with the S_{2n} symmetry of a vertex-bicolored graph; (2) list all "allowed" vertex color motifs; (3) operate with S_{2n} on these motifs to generate the corresponding vertex-bicolored graphs; (4) convert the graph to rigidly achiral presentations. For the purposes of this paper, we limit "allowed" vertex color motifs to those that lead to non-trivial prime knots, i.e., we "disallow" motifs that lead to composite knots, to the unknot, and to linked structures. For example, consider the planar 8-vertex graph in fig. 9, whose innermost and outermost circuits are equivalent. Under the above restriction only one vertex color motif is "allowed"; the operation S_4 on this motif then yields the vertex-bicolored graph for the rigidly achiral presentation of the figure-eight knot [33a,37,11b,d,e].

The 8-vertex knot graph can be expanded to a planar 16-vertex graph with fourfold symmetry by the addition of two concentric squares (fig. 10); once again the
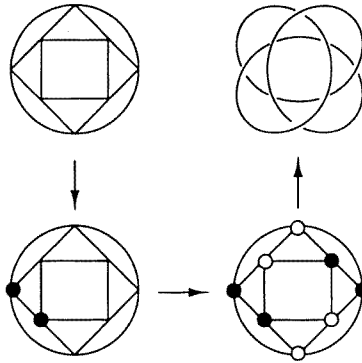
Fig. 9. Conversion of a 8-vertex knot graph to a S_4 presentation of the figure-eight knot. Top left: knot graph with fourfold symmetry. Bottom left: vertex color motif. Bottom right: G(4_1, S_4). Top right: S_4 diagram.
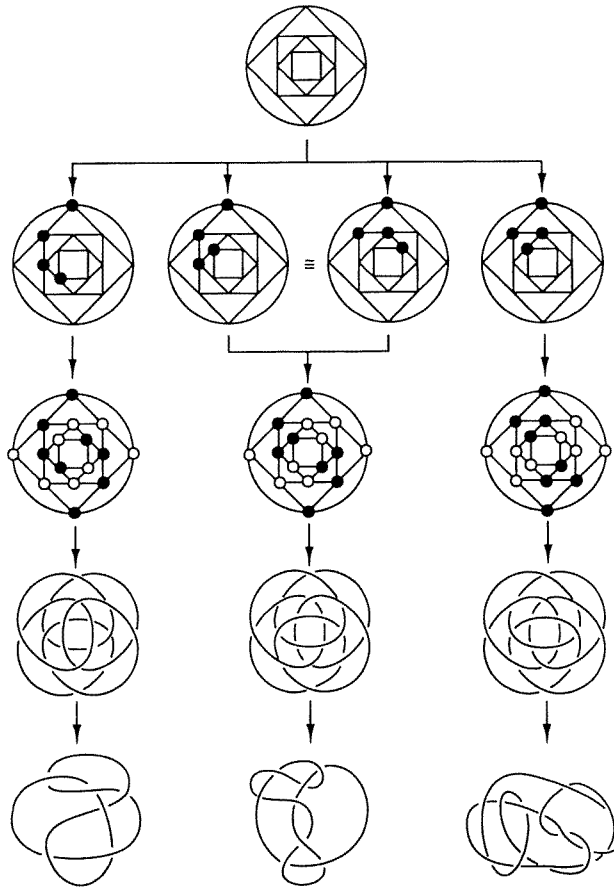
Fig. 10. Conversion of a 16-vertex knot graph with fourfold symmetry (top) to S_4 presentations of 6_3 (left), 8_{12} (center), and a 14-crossing non-alternating prime knot (right). Shown in vertical descent are the respective vertex color motifs, vertex-bicolored knot graphs, S_4 diagrams, and reduced knot diagrams.

innermost and outermost circuits are equivalent. There are now exactly 3 allowed vertex color motifs which, under the operation of S_4, yield vertex-bicolored graphs for the S_4 presentations of 6_3 [32b], 8_{12}, and a 14-crossing non-alternating amphicheiral prime knot. Further expansion, to the 24-vertex knot graph in fig. 11, and selection of 3 out of the 10 allowed vertex color motifs, yields S_4 presentations for 8_9, 10_{43}, and 10_{45}. Finally, expansion to the 32-vertex knot graph in fig. 12 yields the S_4 presentation of 10_{17}; this requires choosing one of 36 allowed vertex color motifs.
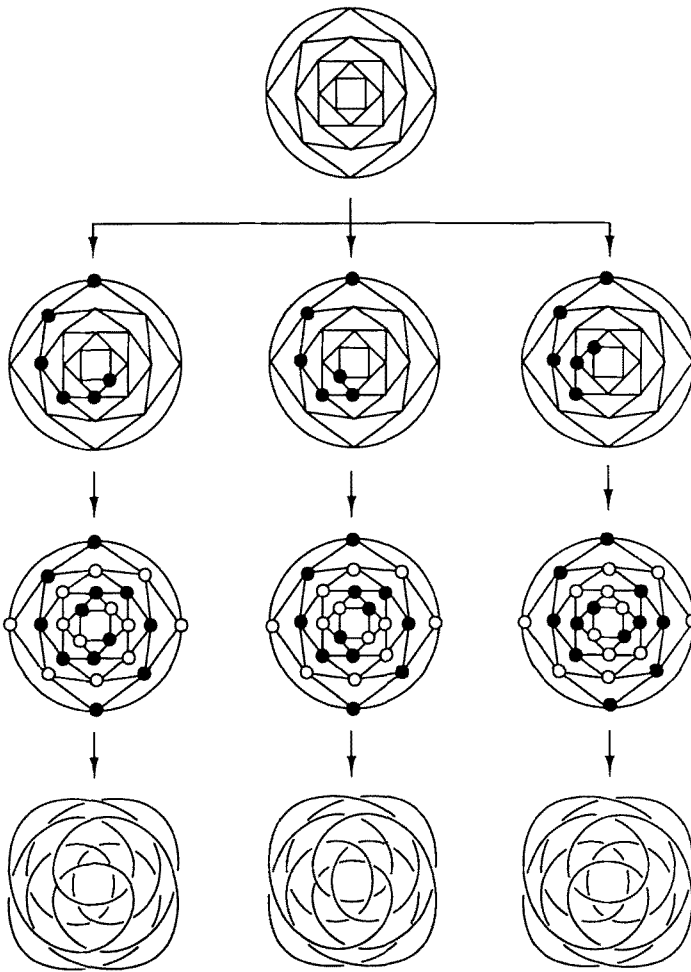
Fig. 11. Conversion of a 24-vertex knot graph (top) to S_4 presentations of 8_9 (left), 10_{43} (center), and 10_{45} (right). Shown in vertical descent are the respective vertex color motifs, vertex-bicolored knot graphs, and S_4 diagrams.
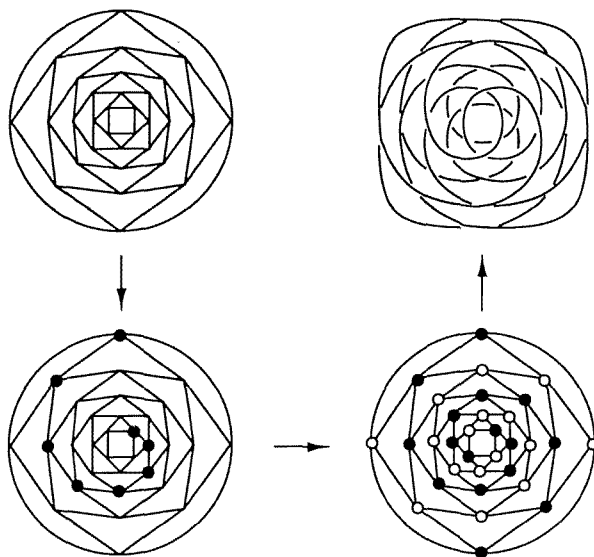
Fig. 12. Conversion of a 32-vertex knot graph to a S_4 presentation of 10_{17}. Top left: knot graph with fourfold symmetry. Bottom left: one of 36 allowed vertex color motifs. Bottom right: $G(10_{17}, S_4)$. Top right: S_4 diagram.

Different types of knot graphs are required for the generation of rigidly achiral presentations of the remaining classical amphicheiral prime knots. Fig. 13 shows conversion of a 12-vertex knot graph into the S_4 presentation of 8_3 by use of the single allowed vertex color motif. Fig. 14 shows two different 20-vertex knot graphs
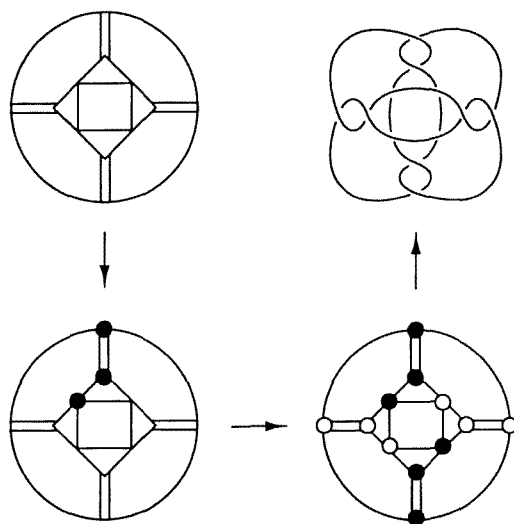
Fig. 13. Conversion of a 12-vertex knot graph to a S_4 presentation of 8_3. Top left: knot graph with fourfold symmetry. Bottom left: vertex color motif. Bottom right: $G(8_3, S_4)$. Top right: S_4 diagram.
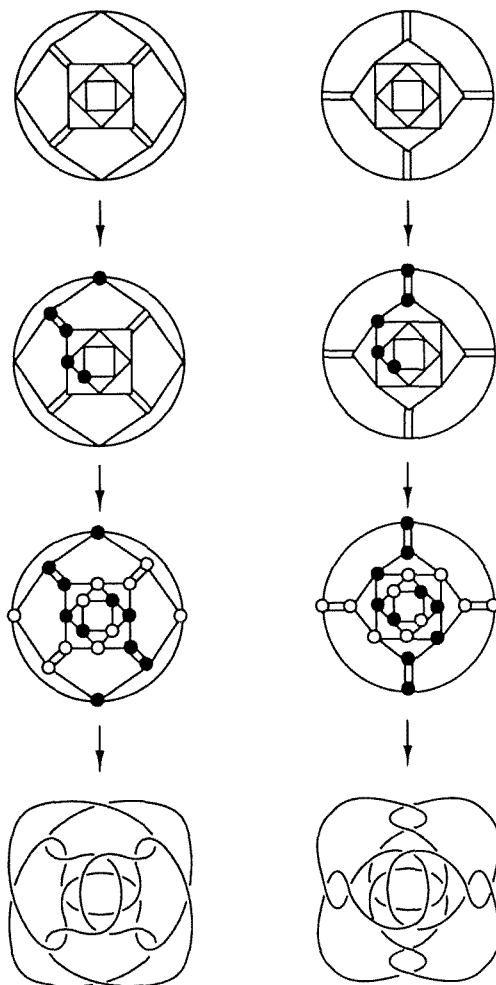
Fig. 14. Conversion of two 20-vertex knot graphs to S_4 presentations of 10_{33} (left) and 10_{37} (right). Shown in vertical descent are the respective vertex color motifs, vertex-bicolored knot graphs, and S_4 diagrams.

that are converted into S_4 presentations of 10_{33} and 10_{37} via, in each case, one of 6 allowed vertex color motifs. And fig. 15 shows a 16-vertex knot graph with eight-fold symmetry that is developed into a S_8 presentation of 8_{18} [32b] by choice of the single allowed vertex color motif.

The remaining two knots, 10_{99} and 10_{123}, are of special interest because their rigidly achiral presentations lack an axis of rotation and thus belong to S_2 ($\equiv C_i$) [33b, 34a]. Fig. 16 shows two different S_2 presentations of 10_{99} and the corresponding 12-vertex bicolored graphs. That a given knot can adopt more than one achiral symmetry is exemplified by the S_{10} presentation of 10_{123} in fig. 17; a beautiful rendering of this knot may be found in [48].
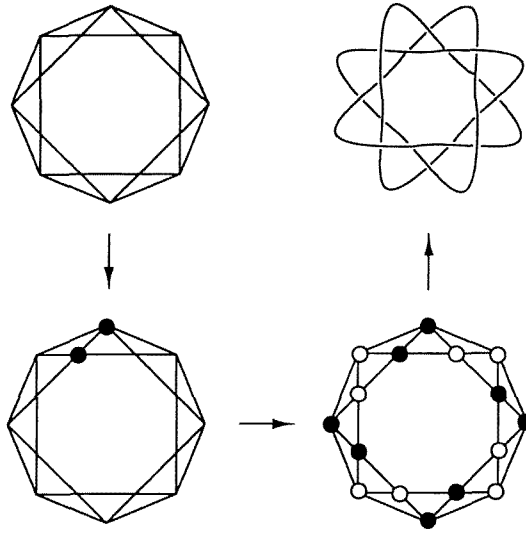
Fig. 15. Conversion of a 16-vertex knot graph with eightfold symmetry to a S_8 presentation of 8_{18}. Top left: knot graph with fourfold symmetry. Bottom left: vertex color motif. Bottom right: $G(8_{18}, S_8)$. Top right: S_8 diagram.

We conclude this section with three observations. First, it is impossible to construct S_{2n} diagrams of the classical amphicheiral prime knots without the addition of nugatory crossings (figs. 9–17). Second, the adjacency matrices $A(K, S_{2n})$ that correspond to S_{2n} diagrams exhibit structures akin to those discussed in section 3.2, as illustrated for $A(4_1, S_4)$ and $A(10_{99}, S_2)$ below. Note that the latter, which corresponds to the diagram at the top of fig. 16, has a minor diagonal that consists entirely of zeros; this is true of all $A(K, S_2)$'s.
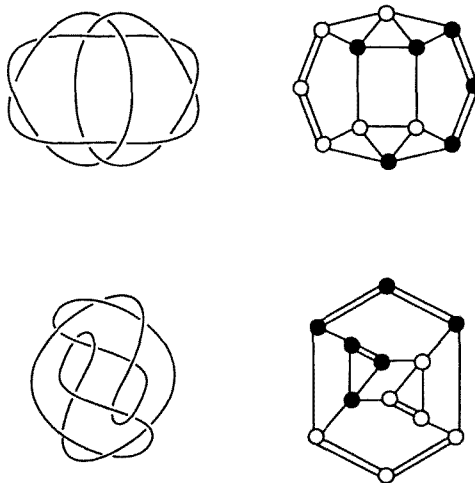
Fig. 16. Two S_2 presentations of 10_{99}. Left: diagrams. Right: associated vertex-bicolored knot graphs.
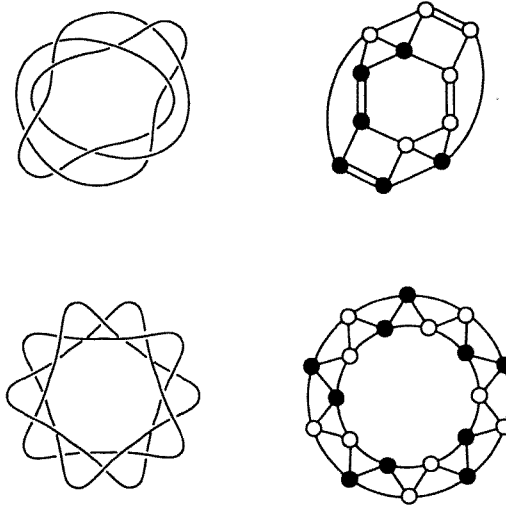
Fig. 17. Two rigidly achiral presentations of 10_{123} and associated vertex-bicolored knot graphs. Top: S_2 symmetry. Bottom: S_{10} symmetry.

$$\mathbf{A}(4_1, S_4) = \begin{pmatrix} t & 0 & 0 & 1 & 1 & 1 & 1 & 0 \\ 0 & t & 1 & 0 & 0 & 1 & 1 & 1 \\ 0 & 1 & t & 0 & 1 & 0 & 1 & 1 \\ 1 & 0 & 0 & t & 1 & 1 & 0 & 1 \\ 1 & 0 & 1 & 1 & t^{-1} & 0 & 0 & 1 \\ 1 & 1 & 0 & 1 & 0 & t^{-1} & 1 & 0 \\ 1 & 1 & 1 & 0 & 0 & 1 & t^{-1} & 0 \\ 0 & 1 & 1 & 1 & 1 & 0 & 0 & t^{-1} \end{pmatrix}$$

$$\mathbf{A}(10_{99}, S_2) = \begin{pmatrix} t & 1 & 0 & 0 & 0 & 0 & 1 & 1 & 1 & 0 & 0 & 0 \\ 1 & t & 2 & 0 & 0 & 0 & 1 & 0 & 0 & 0 & 0 & 0 \\ 0 & 2 & t & 2 & 0 & 0 & 0 & 0 & 0 & 0 & 0 & 0 \\ 0 & 0 & 2 & t & 1 & 0 & 0 & 0 & 0 & 0 & 0 & 1 \\ 0 & 0 & 0 & 1 & t & 1 & 1 & 0 & 0 & 0 & 0 & 1 \\ 0 & 0 & 0 & 0 & 1 & t & 0 & 1 & 0 & 0 & 1 & 1 \\ 1 & 1 & 0 & 0 & 1 & 0 & t^{-1} & 1 & 0 & 0 & 0 & 0 \\ 1 & 0 & 0 & 0 & 0 & 1 & 1 & t^{-1} & 1 & 0 & 0 & 0 \\ 1 & 0 & 0 & 0 & 0 & 0 & 0 & 1 & t^{-1} & 2 & 0 & 0 \\ 0 & 0 & 0 & 0 & 0 & 0 & 0 & 0 & 2 & t^{-1} & 2 & 0 \\ 0 & 0 & 0 & 0 & 0 & 1 & 0 & 0 & 0 & 2 & t^{-1} & 1 \\ 0 & 0 & 0 & 1 & 1 & 1 & 0 & 0 & 0 & 0 & 1 & t^{-1} \end{pmatrix}$$

Third, by purposely restricting the generation of rigidly achiral presentations to non-trivial prime knots, we have severely limited the scope of the combinatorial possibilities inherent in our algorithm: relaxation of this constraint on vertex color motifs yields amphicheiral links, composite knots, and the unknot, in addition to a plethora of prime knots. We have initiated a systematic study of the algorithm in order to explore its full potential.

4.2. WIRE MODELS

Walba [11d] had noted that "Interestingly, a figure-of-eight knot made of wire, such that there is a force tending to give the presentation with the least bending of the 'line', spontaneously springs into the symmetry [S_4] presentation!". For a time this "jumping knot" even became commercially available [49]! Since we had worked out S_{2n} presentations for all of the classical invertible amphicheiral prime knots, it became of some interest to examine the corresponding wire models.

4.2.1. Method of construction

All wire models were constructed as follows: a suitable length of 0.03 in. dia. steel spring wire was bent into a shape with minimum crossings, and the ends were then brought together and fused with silver solder. In the process of bending and fusing, every effort was made to minimize unnecessary strain and to avoid twisting the wire about its long axis. This procedure yielded the "standard model". If one end of the wire was twisted by one or more full turns prior to fusion, the resulting model exhibited nugatory crossings and "abnormal" (relative to the standard model) behavior. For example, the standard model of the figure-eight knot behaves exactly as described by Walba: first compressed into a flat circular pile and then released, the model jumps as it assumes a rounded S_4 conformation, with two + crossings at one end and two − crossings at the other. But a wire model of the trefoil knot with one extra (nugatory) crossing, obtained by twisting one end of the wire by a full turn prior to fusion, behaves in *exactly* the same manner, only now the jumping knot has D_2 symmetry, with two + or two − crossings at *both* ends. Similarly, a wire model of the figure-eight knot with one extra crossing has C_2 symmetry, with three + (or −) crossings at one end and two − (or +) at the other.

4.2.2. Higher homologues of the amphicheiral jumping knot

With the sole exception of 4_1 and 8_3, none of the standard wire models of the 13 invertible amphicheiral prime knots with up to 10 crossings showed the slightest tendency spontaneously to adopt rigidly achiral presentations. What 4_1 and 8_3 have in common is that they are members of a homologous series of amphicheiral knots with $c(K) = 4n, n = 1, 2, \ldots$, whose S_4 diagrams have $4(n+1)$ minimum crossings. Indeed, wire models of the appropriate knots with $c(K) = 12, 16$, and 20 also spontaneously adopted the corresponding S_4 presentations (fig. 18). The family relationship is summarized schematically in fig. 19.
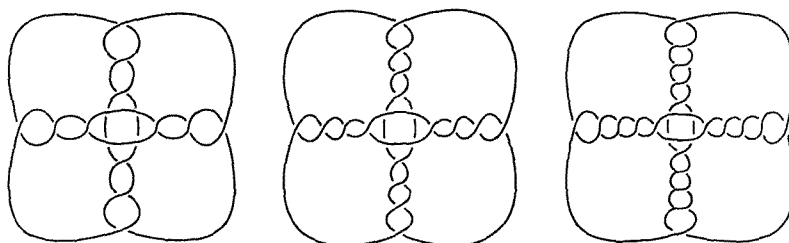
Fig. 18. S_4 diagrams of knots with $c(K) = 12$ (left), 16 (center), and 20 (right), corresponding to vertex-bicolored knot graphs #3, 4, and 5 in fig. 19.

As $c(K)$ increases, the models become elongated along the S_4 axis. Wire models of knots with $c(K) \geqslant 12$ are quite flexible, and upon compression along the S_4 axis spring into a new conformation in which one half of the model has turned inside out to produce a bowl-shaped entity with C_2 symmetry. Flattening this bowl produces one of two results: either the model pops back into the original S_4 shape, or it inverts directly into its mirror image. The two paths are illustrated in fig. 20 for a 16-crossing knot. These processes bear a formal resemblance to the bowl-to-bowl inversion of corannulene [50] and the tub-to-tub inversion of cyclooctatetraene [51] – even to the extent that direct inversion of the wire model has the same "feel" as inversion of a Dreiding model of cyclooctatetraene. The interconversions in fig. 20 are thus formally analogous to direct and indirect (via an achiral intermediate) unimolecular enantiomerization processes, as illustrated by the energy profile in fig. 20. It is also the case that the relative energies of conformations A (or C) and B crucially depend on the crossing number. Thus, the S_4 conformation is the only accessible energy minimum for models of 4_1 and 8_3, while A and C are shallow minima for models of the 12-crossing knot in fig. 18. Only for models of knots with
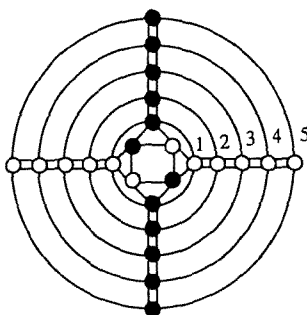
Fig. 19. Schematic diagram showing the first five members of a family of vertex-bicolored knot graphs associated with S_4-symmetric presentations. #1 = 8-vertex graph for 4_1; #2 = 12-vertex graph for 8_3; #3 = 16-vertex graph for a knot with $c(K) = 12$; #4 = 20-vertex graph for a knot with $c(K) = 16$; #5 = 24-vertex graph for a knot with $c(K) = 20$. Four edges form a circle on the outside of each graph; inside circles must be suppressed for 8_3 and higher knots.
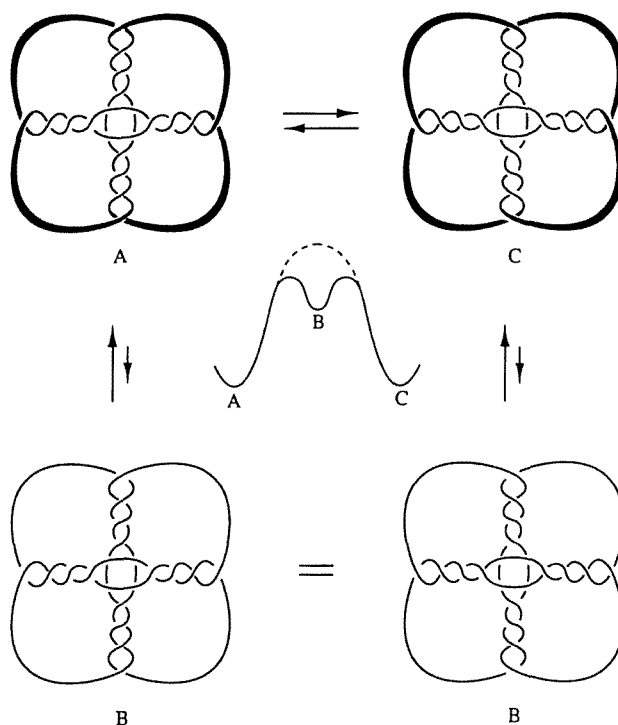
Fig. 20. Wire model of the 16-crossing knot in fig. 18. Top left and right: diagrams of enantiomorphous bowl- shaped models with C_2 symmetry (A and C) viewed along the C_2 axis. Heavy shading indicates that the rim of the bowl is close to the observer. Bottom: diagram of model with S_4 symmetry (B) viewed along the S_4 axis. Center: schematic sketch of an energy profile for the interconversion ("enantiomerization") of A and C. The dashed line indicates one-step interconversion through a "transition state" and the solid line two-step interconversion through an "intermediate".

$c(K) > 12$ do the enantiomorphous bowl conformations A and C acquire a significant measure of stability.

Extensions to non-amphicheiral knots are readily envisaged: addition or subtraction of one or more crossings at one end of the S_4 axis desymmetrizes the S_4 wire model to one with C_2 symmetry. The bowls in this model are no longer related by symmetry, as illustrated for a 18-crossing knot in fig. 21, and the bowl-to-bowl interconversions are now formally analogous to diastereomerization processes.

5. The 12-crossing amphicheiral prime knots

Knots with up to 10 crossings have been thoroughly studied over a period of more than a century. In contrast, knots with crossing numbers in excess of 10 are, for all intents and purposes, terra incognita. As regards amphicheiral prime knots with $c(K) > 10$, to our knowledge there exists only one published tabulation of 12-crossing amphicheirals, by Haseman [52], and one that is still unpublished, by Thistlethwaite [53]. No tabulations exist for amphicheiral knots with $c(K) > 12$.
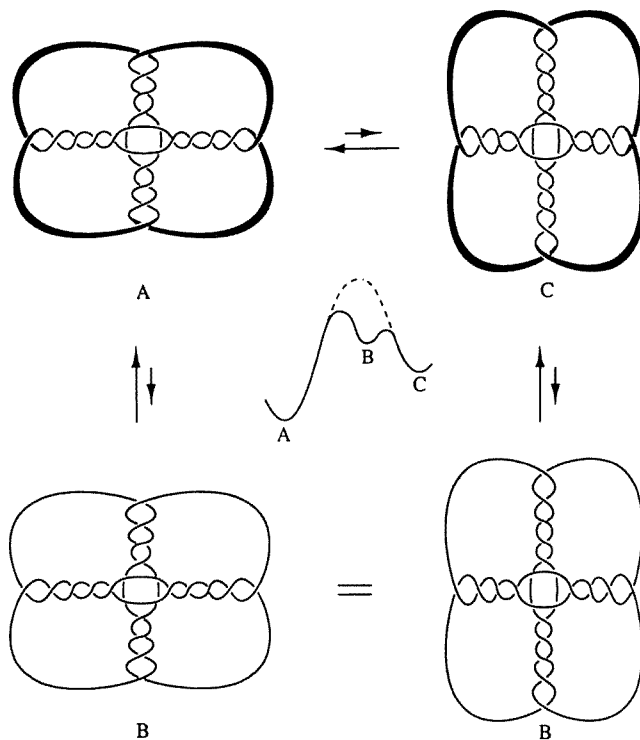
Fig. 21. Wire model of a non-amphicheiral 18-crossing knot obtained by addition of two crossings to one end of the S_4 axis of the 16-crossing knot in fig. 20. A diagram of the resulting model with C_2 symmetry (B) is shown at the bottom, viewed along the C_2 axis. Top left and right: diagrams of anisometric bowl-shaped models with C_2 symmetry (A and C), viewed along the C_2 axis. Heavy shading indicates that the rim of the bowl is close to the observer. Center: schematic sketch of an energy profile for interconversion ("diastereomerization") of A and C. The dashed and solid lines have the same significance as in fig. 20.

5.1. CENSUS OF 12-CROSSING AMPHICHEIRALS

Haseman used Tait's empirical methods to extend the list of amphicheirals to the 61 alternating knots with 12 crossings whose projections are shown in fig. 22 (reproduced from [52]). In what follows, we denote these knots by H_n, where n is the number given in fig. 22; where appropriate, we add, in parentheses, Thistlethwaite's corresponding (and as yet unpublished) 12_n notation.

As Thistlethwaite has pointed out [20], and as we were able to confirm, there are 7 duplications in Haseman's list: $H_{16} = H_{13}$, $H_{36} = H_{20}$, $H_{51} = H_{50}$, $H_{54} = H_{40}$, $H_{57} = H_{45}$, $H_{60} = H_{59}$, and $H_{61} = H_6$. Furthermore, three of the knots in fig. 22 (H_{10} and $H_{59} = H_{60}$) are shown in projections of diagrams that lack the twofold antisymmetry characteristic of amphicheirals. We return to the case of H_{59} and H_{60} in section 5.3; here we merely point out that the projection shown for H_{10} in [52] corresponds to that of a *chiral* knot, writhe 4. The problem may be traced to an error in the last letter of Haseman's alphabetical symbol for H_{10}, *chagkidbflek*. The

MARY G. HASEMAN: AMPHICHEIRAL KNOTS OF TWELVE CROSSINGS.
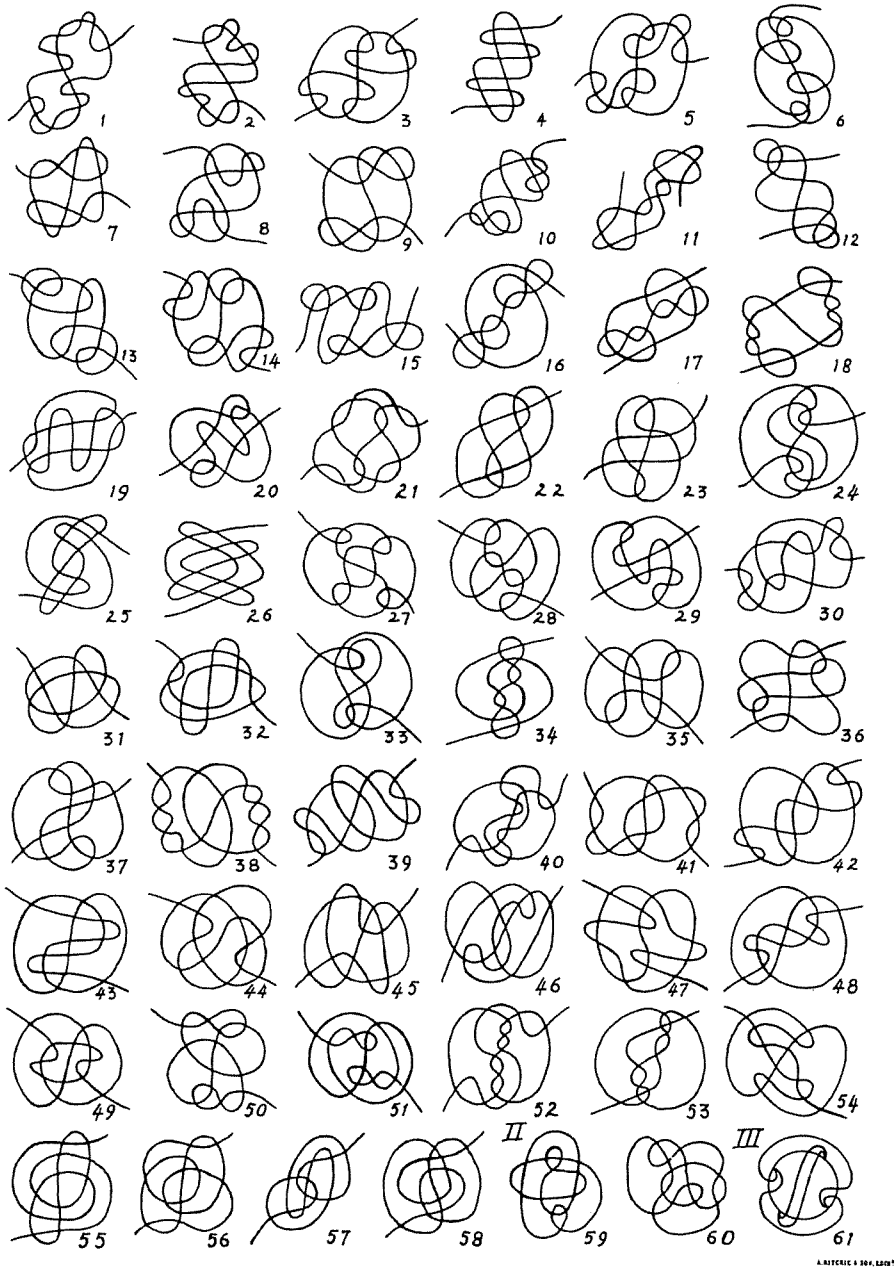
Fig. 22.

correct symbol, *chagkidbflej*, corresponds to the Tait diagram of the amphicheiral knot 12_{477} depicted in fig. 23(a), which should therefore be substituted for H_{10} in fig. 22.

(a)   (b)
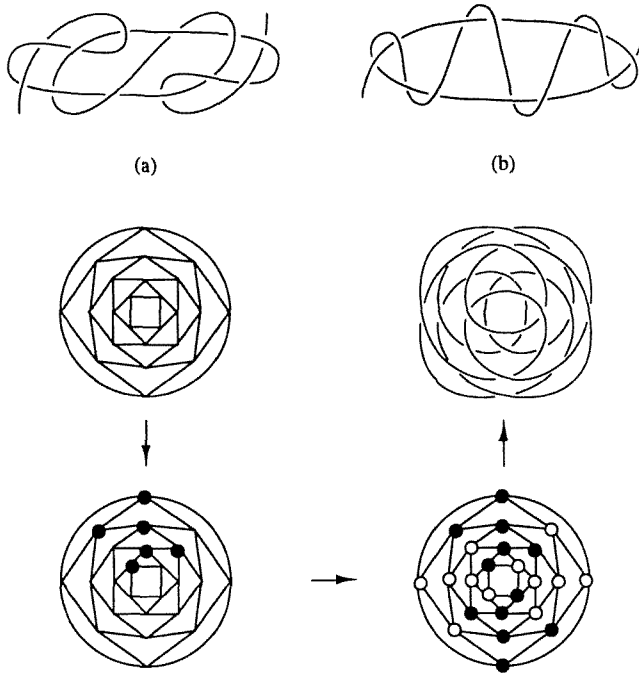
Fig. 23. Top: two different Tait diagrams of knot 12_{477}. Bottom: conversion of the 24-vertex knot graph in fig. 11 to a S_4 presentation of 12_{477}. Shown in anticlockwise order: knot graph, vertex color motif, $G(12_{477}, S_4)$, S_4 diagram.

In addition to the $61 - 7 = 54$ alternating knots, there are 4 that are non-alternating [53] and that are depicted in fig. 24. These are the smallest non-alternating amphicheiral prime knots, but there are obviously many more non-alternating amphicheirals among knots with higher crossing numbers (e.g., see fig. 10).

12_{1644} 12_{1750}

12_{1994} 12_{2161}
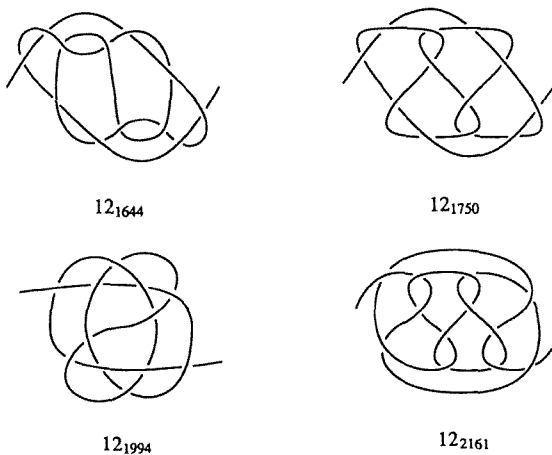
Fig. 24. Tait diagrams of the four non-alternating amphicheiral prime knots with $c(K) = 12$.

5.2. RIGIDLY ACHIRAL PRESENTATIONS

Presentations of 12-crossing prime amphicheirals with S_{2n} symmetry can be derived by use of the algorithm described in section 4.1. Thus, the S_4 diagram of $H_1(12_{1287})$ is depicted on the left in fig. 18, and its vertex-bicolored graph is #3 in fig. 19. Starting with the 24-vertex knot graph in fig. 11, use of one of the 10 allowed vertex color motifs leads to the S_4 diagram of 12_{477} (fig. 23, bottom). Similarly, starting with the 20-vertex knot graphs in fig. 14, use of one of the 6 vertex color motifs allowed for each leads to the S_4 diagrams of $H_{11}(12_{1127})$ and $H_{18}(12_{471})$ (fig. 25).
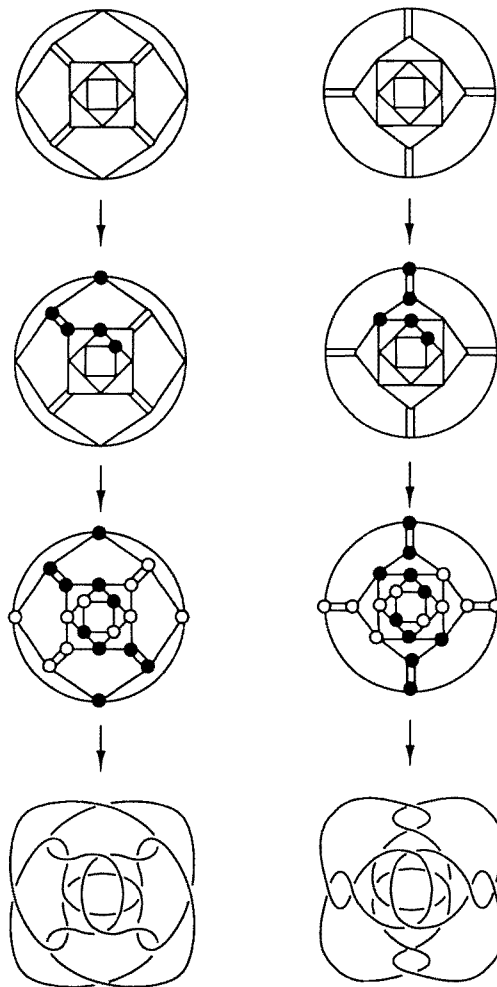
Fig. 25. Conversion of the two 20-vertex knot graphs in fig. 14 to S_4 presentations of $H_{11}(12_{1127})$ (left) and $H_{18}(12_{471})$ (right). Shown in vertical descent are the respective vertex color motifs, vertex-bicolored knot graphs, and S_4 diagrams.
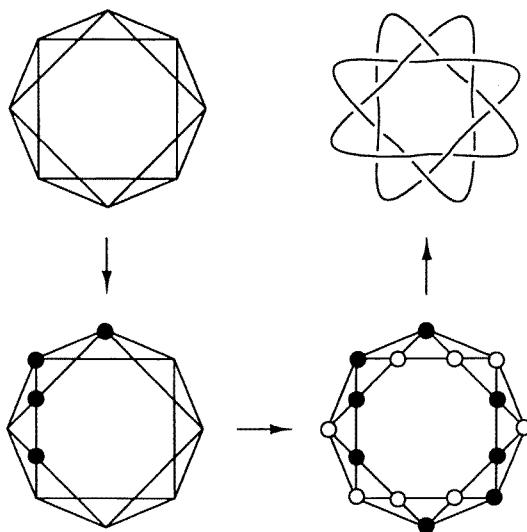
Fig. 26. Conversion of the 16-vertex knot graph in fig. 15 to a S_4 presentation of $H_3(12_{1288})$. Top left: knot graph with fourfold symmetry. Bottom left: vertex color motif. Bottom right: vertex-bicolored knot graph. Top right: S_4 diagram.

As an example of how different vertex color motifs may lead from the same knot graph to different symmetries, consider the 16-vertex knot graph in fig. 15: one motif leads to the S_8 diagram of 8_{18} (fig. 15) while another leads to the S_4 diagram of $H_3(12_{1288})$ (fig. 26). In each case, the corresponding motif is the only one allowed for that symmetry.
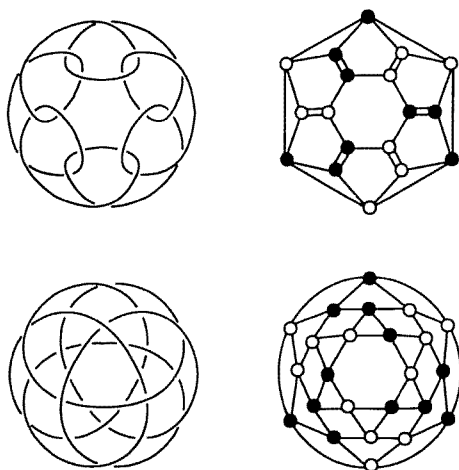
Fig. 27. Diagrams of rigid achiral presentations with S_6 symmetry, and their vertex-bicolored graphs. Top: $H_{21}(12_{1202})$. Bottom: $H_{22}(12_{1019})$.
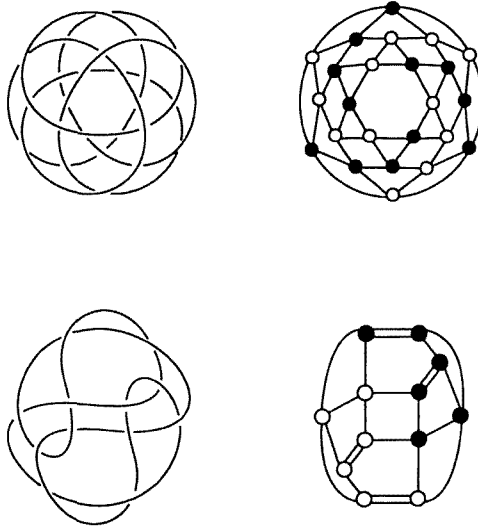
Fig. 28. Diagrams of two rigidly achiral presentations of the non-alternating knot 12_{1994}, and their vertex-bicolored graphs. Top: S_6 symmetry, 24 crossings. Bottom: S_2 symmetry, 12 crossings.

We find that 12-crossing amphicheirals are the smallest knots to support presentations with S_6 symmetry; two examples are shown in fig. 27 and one in fig. 28. Together with the information contained in section 4.1, this demonstrates the availability of presentations with symmetries $S_{2n}, n = 1, 2, 3, 4$, and 5; examples with higher symmetries are easily produced by the method described in this paper.

One of the rigidly achiral presentations of the non-alternating knot 12_{1994} (fig. 28) is of exceptional interest: the S_2 diagram has only 12 crossings! To our knowledge, this is the first, and so far the only, example of an amphicheiral *prime* knot whose S_{2n} diagram is also a reduced diagram. For *composite* knots this is of course well precedented; the simplest example is the square knot, which is also non-alternating and whose centrosymmetric (C_{2h}) diagram with 6 crossings is also a reduced diagram. To complete the analogy: just as the presentation of 12_{1994} with twofold antisymmetry in fig. 24 can be isotoped to the rigidly achiral presentation in fig. 28, so can the presentation of the square knot with twofold antisymmetry in fig. 29 be isotoped to the rigidly achiral presentation in fig. 1(f).
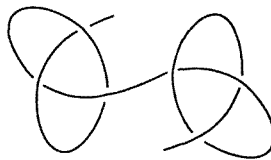
Fig. 29. Tait diagram of the square knot.

5.3. DISCERNIBLE AND CONCEALED ANTISYMMETRY

With a single exception, all amphicheiral prime knots with up to 12 crossings are capable of being shaped into presentations with twofold antisymmetry. The exception is the alternating knot $H_{59} = H_{60}(12_{427})$ (fig. 22 and 30). However, because the connectivities between the black and white subgraphs of $G(H_{59})$ and $G(H_{60})$ in fig. 30 are equivalent, the twofold antisymmetry is revealed in the structures of the respective adjacency matrices and in the corresponding polynomials:

$$\mathbf{A}(H_{59}) = \begin{pmatrix}
t & 1 & 0 & 1 & 0 & 0 & 1 & 1 & 0 & 0 & 0 & 0 \\
1 & t & 2 & 0 & 0 & 1 & 0 & 0 & 0 & 0 & 0 & 0 \\
0 & 2 & t & 1 & 0 & 1 & 0 & 0 & 0 & 0 & 0 & 0 \\
1 & 0 & 1 & t & 2 & 0 & 0 & 0 & 0 & 0 & 0 & 0 \\
0 & 0 & 0 & 2 & t & 0 & 1 & 0 & 0 & 0 & 0 & 1 \\
0 & 1 & 1 & 0 & 0 & t & 0 & 1 & 0 & 0 & 0 & 1 \\
1 & 0 & 0 & 0 & 1 & 0 & t^{-1} & 0 & 0 & 1 & 1 & 0 \\
1 & 0 & 0 & 0 & 0 & 1 & 0 & t^{-1} & 2 & 0 & 0 & 0 \\
0 & 0 & 0 & 0 & 0 & 0 & 0 & 2 & t^{-1} & 1 & 0 & 1 \\
0 & 0 & 0 & 0 & 0 & 0 & 1 & 0 & 1 & t^{-1} & 2 & 0 \\
0 & 0 & 0 & 0 & 0 & 0 & 1 & 0 & 0 & 2 & t^{-1} & 1 \\
0 & 0 & 0 & 0 & 1 & 1 & 0 & 0 & 1 & 0 & 1 & t^{-1}
\end{pmatrix}$$

$$P(t) = P(t^{-1}) = -4t^{-6} - 6t^{-5} + 49t^{-4} + 18t^{-3} - 113t^{-2} + 68t^{-1} - 19$$
$$- 4t^{6} - 6t^{5} + 49t^{4} + 18t^{3} - 113t^{2} + 68t,$$

$$\mathbf{A}(H_{60}) = \begin{pmatrix}
t & 2 & 0 & 0 & 0 & 0 & 0 & 1 & 0 & 1 & 0 & 0 \\
2 & t & 1 & 0 & 0 & 0 & 0 & 0 & 1 & 0 & 0 & 0 \\
0 & 1 & t & 0 & 0 & 0 & 1 & 0 & 1 & 0 & 0 & 1 \\
0 & 0 & 0 & t & 0 & 0 & 1 & 1 & 0 & 1 & 1 & 0 \\
0 & 0 & 0 & 0 & t & 2 & 0 & 0 & 1 & 0 & 0 & 1 \\
0 & 0 & 0 & 0 & 2 & t & 0 & 0 & 1 & 1 & 0 & 0 \\
0 & 0 & 1 & 1 & 0 & 0 & t^{-1} & 2 & 0 & 0 & 0 & 0 \\
1 & 0 & 0 & 1 & 0 & 0 & 2 & t^{-1} & 0 & 0 & 0 & 0 \\
0 & 1 & 1 & 0 & 1 & 1 & 0 & 0 & t^{-1} & 0 & 0 & 0 \\
1 & 0 & 0 & 1 & 0 & 1 & 0 & 0 & 0 & t^{-1} & 1 & 0 \\
0 & 0 & 0 & 1 & 0 & 0 & 0 & 0 & 0 & 1 & t^{-1} & 2 \\
0 & 0 & 1 & 0 & 1 & 0 & 0 & 0 & 0 & 0 & 2 & t^{-1}
\end{pmatrix}$$
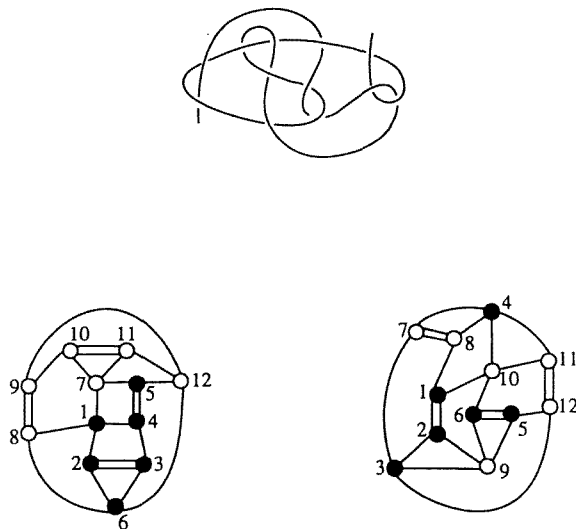
Fig. 30. Top: reduced diagram of $H_{59} = H_{60}(12_{427})$. Bottom: $G(H_{59})$ (left) and $G(H_{60})$ (right). The numbering of vertices refers to the corresponding adjacency matrices in the text.

$$P(t) = P(t^{-1}) = 108t^{-4} - 204t^{-3} - 340t^{-2} + 594t^{-1} - 19$$
$$108t^4 - 204t^3 - 340t^2 + 594t.$$

In all previously discussed cases the twofold antisymmetry was manifest in the presentations themselves; we call this *discernible antisymmetry*. In $H_{59} = H_{60}(12_{427})$, the twofold antisymmetry is not discernible in the knot's presentation but surfaces in the corresponding adjacency matrices; we call this *concealed antisymmetry*. Rigidly achiral presentations of this knot are depicted in fig. 31.
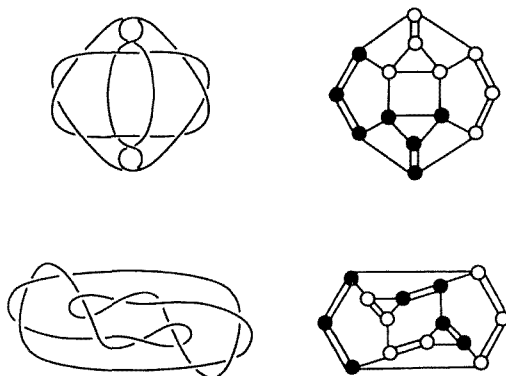
Fig. 31. Diagrams of two rigidly achiral presentations of $H_{59} = H_{60}(12_{427})$ with S_2 symmetry, and their vertex-bicolored graphs.

6. Epilogue

The appeal of amphicheiral knots lies in their special symmetry properties, but in selecting this class of objects we have narrowed our focus on a minuscule subset of topological figures: amphicheiral knots constitute a mere 0.6% of all prime knots with up to 13 crossings. Furthermore, we have totally ignored the universe of complex knots, links, and graphs. Not only that, but our approach has been empirical and intuitive: we have offered neither theorems nor proofs, merely observations and conjectures. Yet, in partial extenuation, "We might allow our thoughts to occasionally escape from the chains of rigor, and, in their freedom, to discover new pathways through the forest" [54].

We close with some comments on the term "amphicheiral", which was introduced and defined in Tait's first paper [29a]. It is significant that Tait's work on knots was stimulated by William Thomson's theory of vortex atoms [55], that Thomson, in 1873, used the terms "homocheiral" and "heterocheiral" [56], and that it was only later, as Lord Kelvin, that Thomson introduced and defined "chiral" and "chirality" [57]. "Homocheiral", "heterocheiral", and "amphicheiral" are therefore contemporaneous coinages that predate "chiral" and whose roots are closer to the original ($\chi\epsilon\iota\rho$ = hand). Furthermore, unlike "achiral", which simply means "not chiral", the prefix ($\alpha\mu\varphi\iota$ = on both sides) in "amphicheiral" is an explicit expression of the twofold antisymmetry (Tait's "quasi-symmetry") that characterizes topologically achiral knots. Finally, "amphicheiral" has its use in applications where topological achirality must not be confused with chemical achirality; for example, single-stranded DNA tied into a figure-eight knot [12c], like circular unknotted DNA, is chiral in all of its chemical and physical manifestations but is nevertheless amphicheiral. However, it should also be noted that the terms "amphicheiral" and "non-amphicheiral" are inappropriate with reference to topologically achiral and chiral non-planar graphs, as, for example, in the case of the topologically achiral Kuck K_5 molecule [58] and the topologically chiral Simmons–Paquette K_5 molecule [59], both of which contain only one (minimum) crossing. In short, "topologically achiral/chiral" subsumes "amphicheiral/non-amphicheiral" since the latter terms are suitably applied only to knots and links.

References

[1] L.L. Liu, R.E. Depew and J.C. Wang, J. Mol. Biol. 106 (1976) 439.

[2] J.C. Wang, Sci. Amer. 247/7 (1982) 94.

[3] M.A. Krasnow, A. Stasiak, S.J. Spengler, F. Dean, T. Koller and N.R. Cozzarelli, Nature 304 (1983) 559.

[4] S.E. Wasserman and N.R. Cozzarelli, Proc. Nat. Acad. Sci. U.S.A. 82 (1985) 1079;
S.E. Wasserman and N.R. Cozzarelli, Science 232 (1986) 951, and references therein;
J.H. White, K.C. Millett and N.R. Cozzarelli, J. Mol. Biol. 197 (1987) 585.

[5] W.J. Ambs, Mendel Bull. 17/Spring (1953) 26.

[6] G. Schill, *Catenanes, Rotaxanes, and Knots* (Academic Press, New York, 1971) p. 18;
G. Schill, R. Henschel and J. Boeckmann, Liebigs Ann. Chem. (1974) 709;
J. Boeckmann and G. Schill, Tetrahedron 30 (1974) 1945.

[7] C.O. Dietrich-Buchecker and J.-P. Sauvage, Angew. Chem. Int. Ed. Engl. 28 (1989) 189;
C.O. Dietrich-Buchecker, J. Guilhem, C. Pascard and J.-P. Sauvage, Angew. Chem. Int. Ed. Engl. 29 (1990) 1154;
J.-P. Sauvage, Acc. Chem. Res. 23 (1990) 319;
Ch. Dietrich-Buchecker and J.P. Sauvage, New J. Chem. 16 (1992) 277;
C.O. Dietrich-Buchecker, J.-P. Sauvage, J.-P. Kintzinger, P. Maltèse, C. Pascard and J. Guilhem, New J. Chem. 16 (1992) 931;
C. Dietrich-Buchecker and J.-P. Sauvage, Bull. Soc. Chim. Fr. 129 (1992) 113.

[8] H.L. Frisch and E. Wasserman, J. Amer. Chem. Soc. 83 (1961) 3789;
E. Wasserman, Sci. Amer. 207/5 (1962) 94.

[9] J. Simon, Proc. Symp. Appl. Math. 45 (1992) 97;
J. Simon, A topological approach to the stereochemistry of nonrigid molecules, in: *Graph Theory and Topology in Chemistry*, eds. R.B. King and D.H. Rouvray (Elsevier, Amsterdam, 1987) pp. 43–75.

[10] V.I. Sokolov, Russ. Chem. Revs. 42 (1973) 452.

[11] (a) D.M. Walba, Stereochemical topology, in: *Chemical Applications of Topology and Graph Theory*, ed. R.B. King (Elsevier, Amsterdam, 1983) pp. 17–32;
(b) D.M. Walba, Tetrahedron 41 (1985) 3161;
(c) D.M. Walba, J.D. Armstrong III, A.E. Perry, R.M. Richards, T.C. Homan and R.C. Haltiwanger, Tetrahedron 42 (1986) 1883;
(d) D.M. Walba, Topological stereochemistry: Knot theory of molecular graphs, in: *Graph Theory and Topology in Chemistry*, eds. R.B. King and D.H. Rouvray (Elsevier, Amsterdam, 1987) pp. 23–42;
(e) D.M. Walba, A topological hierarchy of molecular chirality and other tidbits in topological stereochemistry, in: *New Developments in Molecular Chirality*, ed. P.G. Mezey (Kluwer Acad. Publ., Dordrecht, 1991) pp. 119–129;
(f) D.M. Walba, Q.Y. Zheng and K. Schilling, J. Amer. Chem. Soc. 114 (1992) 6259.

[12] (a) J.E. Mueller, S.M. Du and N.C. Seeman, J. Amer. Chem. Soc. 113 (1991) 6306;
(b) N.C. Seeman, Mol. Eng. 2 (1992) 297;
(c) S.M. Du and N.C. Seeman, J. Amer. Chem. Soc. 114 (1992) 9652.

[13] G. Bain, *Celtic Art: The Methods of Construction* (Dover, New York, 1973);
P.R. Cromwell, The Mathematical Intelligencer 15 (1993) 36, and references therein.

[14] K. Reidemeister, *Ergebnisse der Mathematik Vol. 1: Knotentheorie* (Springer-Verlag, Berlin, 1932) pp. 1–74.

[15] R.H. Fox, A quick trip through knot theory, in: *Topology of 3-Manifolds*, ed. M.K. Fort, Jr. (Prentice Hall, Englewood Cliffs, NJ, 1962) pp. 120–167.

[16] R.H. Crowell and R.H. Fox, *Introduction to Knot Theory* (Blaisdell, New York, 1963).

[17] J.H. Conway, An enumeration of knots and links, and some of their algebraic properties, in: *Computational Problems in Abstract Algebra*, ed. J. Leech (Pergamon Press, New York, 1970) pp. 329–358.

[18] L. Neuwirth, Sci. Amer. 240/6 (1979) 110.

[19] G. Burde and H. Zieschang, *Knots* (Walter de Gruyter, Berlin, 1985), Appendix C: Tables, pp. 311–343.

[20] M.B. Thistlethwaite, Knot tabulations and related topics, in: *Aspects of Topology*, London Math. Soc. Lecture Note Series no. 93, eds. I.M. James and E.H. Kronheimer (Cambridge University Press, Cambridge, 1985) pp. 1–76.

[21] L.H. Kauffman, *On Knots* (Princeton University Press, Princeton, 1987), Knot Tables, pp. 444–473.

[22] J. Simon, A friendly introduction to knot theory, in: *MATH/CHEM/COMP 1987*, ed. R.C. Lacher (Elsevier, Amsterdam, 1988) pp. 37–66.

[23] D.W. Sumners, The knot enumeration problem, in: *MATH/CHEM/COMP 1987*, ed. R.C. Lacher (Elsevier, Amsterdam, 1988) pp. 67–82.

[24] D. Rolfsen, *Knots and Links* (Publish or Perish, Berkeley, 1976; second printing with corrections: Publish or Perish, Houston, 1990), Appendix C: Table of knots and links, pp. 388–429.

[25] J.W. Alexander and G.B. Briggs, On types of knotted curves, Ann. Math. 28 (1926-27) 562–586.

[26] P.G. Mezey, J. Amer. Chem. Soc. 108 (1986) 3976;
D. Tavernier, J. Chem. Educ. 69 (1992) 627.

[27] T.P. Kirkman, The enumeration, description, and construction of knots of fewer than ten crossings, Trans. Roy. Soc. Edin. 32 (1884) 281–309.

[28] C.N. Little, On knots, with a census for order ten, Trans. Conn. Acad. Sci. 7 (1885) 27–43;
C.N. Little, Alternate±knots of order eleven, Trans. Roy. Soc. Edin. 36 (1890) 253–255;
C.N. Little, Non-alternate±knots, Trans. Roy. Soc. Edin. 39 (1898-99) 771–778.

[29] (a) P.G. Tait, On knots, Trans. Roy. Soc. Edin. 28 (1876-77) 145–190;
(b) P.G. Tait, On knots. Part II, Trans. Roy. Soc. Edin. 32 (1884) 327–342;
(c) P.G. Tait, On knots. Part III, Trans. Roy. Soc. Edin. 32 (1885) 493–506;
(d) P.G. Tait, On knots I, II, III, *Scientific Papers Vol. I* (Cambridge University Press, London, 1898) pp. 273–347.

[30] D.W. Sumners, J. Math. Chem. 1 (1987) 1.

[31] J.B. Listing, *Vorstudien zur Topologie. Göttinger Studien 1847* (Vandenhoeck and Ruprecht, Göttingen, 1848) pp. 3–68.

[32] (a) J.M. van Buskirk, Notices Amer. Math. Soc. 177 (1977) A354;
(b) J.M. van Buskirk, Notices Amer. Math. Soc. 26 (1979) A251.

[33] (a) E. Flapan, Pac. J. Math. 129 (1987) 57;
(b) E. Flapan, Topological techniques to detect chirality, in: *New Developments in Molecular Chirality*, ed. P.G. Mezey (Kluwer Acad. Publ., Dordrecht, 1991) pp. 209–239.

[34] (a) R. Hartley and A. Kawauchi, Polynomials of amphicheiral knots, Math. Ann. 243 (1979) 63;
(b) R.I. Hartley, Math. Ann. 252 (1980) 103.

[35] A. Kawauchi, Proc. Jap. Acad. 55, Ser. A (1979) 399.

[36] K.C. Millett, Croat. Chem. Acta 59 (1986) 669.

[37] K.C. Millett, Algebraic topological indices of molecular chirality, in: *New Developments in Molecular Chirality*, ed. P.G. Mezey (Kluwer Acad. Publ., Dordrecht, 1991) pp. 165–207.

[38] J. Simon, Topology 25 (1986) 229;
J. Simon, J. Comput. Chem. 8 (1987) 718.

[39] K. Murasugi, Topology 26 (1987) 187.

[40] M.B. Thistlethwaite, Topology 27 (1988) 311.

[41] A.V. Shubnikov, Symmetry and antisymmetry of finite figures, in: A.V. Shubnikov and N.V. Belov, *Colored Symmetry*, ed. W.T. Holser (Macmillan, New York, 1964) pp. 1–172.

[42] C. Liang and Y. Jiang, J. Theor. Biol. 158 (1992) 231.

[43] T.A. Brown, A note on some graphs related to knots, J. Combin. Theory 1 (1966) 498–502; F. Harary and E.M. Palmer, *Graphical Enumeration* (Academic Press, New York, 1973) pp. 231–233.

[44] J.W. Alexander, Topological invariants of knots and links, Trans. Amer. Math. Soc. 30 (1928) 275–306.

[45] V.F.R. Jones, Bull. Amer. Math. Soc. 12 (1985) 103.

[46] P. Freyd, D. Yetter, J. Hoste, W.B.R. Lickorish, K. Millett and A. Ocneanu, Bull. Amer. Math. Soc. 12 (1985) 239; W.B.R. Lickorish and K.C. Millett, Topology 26 (1987) 107; W.B.R. Lickorish and K.C. Millett, Math. Mag. 61 (1988) 3.

[47] L.H. Kauffman, Amer. Math. Monthly 95 (1988) 195.

[48] S. Wolfrom, *Mathematica: A System for Doing Mathematics by Computer*, 2nd ed. (Addison-Wesley, Redwood City, CA, 1991). Mathematics Graphics Gallery, p. 32.

[49] WHY KNOTS, Box 635, Aptos, CA 95003, USA.

[50] L.T. Scott, M.M. Hashemi and M.S. Bratcher, J. Amer. Chem. Soc. 114 (1992) 1920; A. Borchardt, A. Fuchicello, K.V. Kilway, K.K. Baldridge and J.S. Siegel, J. Amer. Chem. Soc. 114 (1992) 1921.

[51] F.A.L. Anet, A.J.R. Bourn and Y.S. Lin, J. Amer. Chem. Soc. 86 (1964) 3576.

[52] M.G. Haseman, On knots, with a census of the amphicheirals with twelve crossings, Trans. Roy. Soc. Edin. 52 (1918) 235–255.

[53] M.B. Thistlethwaite, unpublished results.

[54] B. Berndt, cited in R. Kanigel, *The Man Who Knew Infinity* (Washington Square Press, New York, 1991) p. 183.

[55] W. Thomson, On vortex atoms, Phil. Mag. 34 (1867) 15–24; W. Thomson, Vortex statics, Proc. Roy. Soc. Edin. 9 (1875-76) 59–73.

[56] W. Thomson, Note on homocheiral and heterocheiral similarity, Proc. Roy. Soc. Edin. 8 (1872-75) 70 [read Feb. 17, 1873, title only].

[57] W.T. Kelvin, *Baltimore Lectures on Molecular Dynamics and the Wave Theory of Light* (C.J. Clay, London, 1904) p. 619 [based on a course of twenty lectures delivered in the late summer of 1884]; W.T. Kelvin, On the molecular tactics of a crystal: *Second Robert Boyle Lecture* (Oxford, 1894). Cited in: L.L. Whyte, Leonardo 8 (1975) 245.

[58] D. Kuck and A. Schuster, Angew. Chem. Int. Ed. Engl. 27 (1988) 1192.

[59] H.E. Simmons III and J.E. Maggio, Tetrahedron Lett. 22 (1981) 287; L.A. Paquette and M. Vazeux, Tetrahedron Lett. 22 (1981) 291.